



Published in final edited form as:

Mol Cancer Ther. 2009 January ; 8(1): 36–44. doi:10.1158/1535-7163.MCT-08-0789.

UA62784; a novel inhibitor of CENP-E kinesin-like protein

Meredith C. Henderson¹, Yeng-Jeng Y. Shaw², Hong Wang³, Haiyong Han³, Laurence H. Hurley^{1,2,4}, Gary Flynn², Robert T. Dorr^{1,4,*}, and Daniel D. Von Hoff³

(1)University of Arizona, Arizona Cancer Center, 1515 N. Campbell Ave., Tucson, AZ 85724-5024

(2)University of Arizona, BIO5 Institute, 1657 E. Helen St. Tucson, AZ 85721-0240

(3)Translational Genomics Research Institute (TGen), 445 N. Fifth Street, 6th Floor, Phoenix, AZ 85004

(4)College of Pharmacy, University of Arizona, 1295 N. Martin, Tucson, AZ 85721

Abstract

Pancreatic carcinoma is the fourth-leading cause of death from cancer. Novel targets and therapeutic options are needed to aid in the treatment of pancreatic cancer. The compound UA62784 is a novel fluorenone with inhibitory activity against the CENP-E kinesin-like protein. UA62784 was isolated due to its selectivity in isogenic pancreatic carcinoma cell lines with a deletion of the DPC4 gene. UA62784 causes mitotic arrest by inhibiting chromosome congression at the metaphase plate, likely through inhibition of the microtubule-associated ATPase activity of CENP-E. Furthermore, CENP-E binding to kinetochores during mitosis is not affected by UA62784, suggesting that the target lies within the motor domain of CENP-E. UA62784 is a novel specific inhibitor of CENP-E and its activity suggests a potential role for antimetabolic drugs in treating pancreatic carcinomas.

Keywords

DPC4; pancreatic; cancer; CENP-E; kinesin

Introduction

Pancreatic carcinoma is the fourth-leading cause of cancer related deaths in the United States today (1). Most patients are diagnosed with advanced disease at a time when very little can be done to extend life expectancy beyond 5-6 months in inoperable cases (for review see (2)). Gemcitabine (Gemzar®) remains the best treatment option, though it only modestly increases survival (3,4). The antimetabolic agent Docetaxel has been used as a potential adjuvant treatment for pancreatic carcinoma, though clinical results comparing gemcitabine-docetaxel combination to gemcitabine alone have been mixed (5-7). Recent work demonstrates that the mitotically active Aurora Kinase (AK) is overexpressed and may comprise a potential target in pancreatic cancer (8). Indeed, the anti-AK drug VX-680 demonstrates potent, selective cytotoxicity and suppression of pancreatic tumor growth in xenografted mice (9). These findings provide support for the use of novel antimetabolic agents in treating pancreatic carcinoma.

During mitosis, paired homologous chromosomes are segregated into two daughter cells through attachment to a bipolar spindle. The formation of a functional bipolar spindle is

*Corresponding author Robert T. Dorr, Ph.D., R. Ph. Professor of Pharmacology Arizona Cancer Center 1515 N. Campbell Ave. Tucson, AZ 85724-5024 T: (520) 626-7892 F: (520) 626-2751.

²Reprint Request Address: Robert T. Dorr, Ph.D., R. Ph. 1515 N. Campbell Ave. Tucson, AZ 85724-5024

absolutely essential to the equitable division of genetic material and failure to form such a structure leads to mitotic arrest and cell death (for review, see (10)). The spindle checkpoint monitors both the attachment of microtubules to the kinetochores and the tension exerted by these attachments (11-13). Only when all kinetochores are attached to opposing poles can anaphase proceed and thereby allow division of the duplicated chromosomes. Agents that prevent this mitotic process from proceeding are referred to as mitotic inhibitors or antimetabolic agents.

Mitotic inhibitors, such as taxanes and vinca alkaloids, have proven to be extremely useful in the treatment of various cancers. However, it is worth noting that the vast majority of mitotic inhibitors target microtubule polymerization and most produce limiting side effects such as neurotoxicity and neutropenia (14,15). Additionally, many of these agents are subject to acquired drug resistance, usually through P-glycoprotein mediated extrusion of drug from the cell (15,16). Recently, the requisite involvement of other mitotic factors (i.e. polo-like kinase 1 (17), Aurora-A kinase (8), and Eg5 kinesin (18)) have sparked interest as potential targets for drug development, especially in developing antimetabolic agents that do not target microtubules (for review, see (19)).

Recently, Monastrol was introduced as a mitotic inhibitor that does not affect tubulin polymerization rather, it blocks mitosis by inhibiting Eg5 Kinesin ATPase activity (20). Monastrol is highly selective for the Eg5 kinesin and is effective in the low nanomolar range (20,21). Additionally, Eg5 has been validated as a molecular target for treatment of various cancers (22-24). Monastrol was the first example of a targeted Eg5 inhibitor. Prior to monastrol, most previously known kinesin inhibitors affected multiple kinesin family members (25). The mitotic kinesin motor proteins such as Eg5 and centromere protein E (CENP-E) are of interest because they are only involved in mitosis and not in neuronal function. Centromere Protein E (CENP-E) is a kinesin-like protein that localizes to the kinetochore during mitosis and is essential for bipolar spindle formation (26,27). The ability of CENP-E to capture microtubules and its association with BubR1 are thought to play a major role in the spindle checkpoint (28). Cells treated with siRNA or injected with antibodies against CENP-E arrest prior to metaphase (27,29,30).

The small molecule UA62784 was isolated from a high-throughput cytotoxicity screen of a commercially-available Nanosyn-based chemical library. The goal was to isolate compounds that selectively targeted DPC4-deleted pancreatic cancer cells (31). Although known to be cytotoxic in the nanomolar range, the mechanism of action for UA62784 was heretofore unknown. We report here that UA62784 causes reversible cell-cycle arrest in mitosis prior to metaphase, with treated cells failing to form a functional bipolar spindle. Treated cells undergo apoptosis and even though UA62784 prevents the formation of a functional bipolar spindle, it does not affect tubulin polymerization nor does it affect certain signal transduction events prior to activation of the anaphase-promoting complex. Finally, we will show that UA62784 causes mitotic arrest by inhibiting the microtubule-associated ATPase activity of the CENP-E kinesin-like protein.

Materials and Methods

UA62784 Synthesis

To obtain sufficient amounts of drug for biological testing, a chemical synthesis of UA62784 was carried out (Figure 1). A solution of 9-oxo-9H-fluorene-4-carboxylic acid (11.21 g, 50.0 mmol) in 150 ml DCM, thionyl chloride (11.90 g, 100.0 mmol) and DMF (0.366 g, 5.0 mmol) was stirred at reflux for 2 hours and evaporated *in vacuo* to remove excess amount of thionyl chloride. The solid residue was dissolved in 200 ml DCM, 2-amino-4'-methoxyacetophenone hydrochloride (8.07g, 90 % purity, 40.0 mmol) was added to the solution and then triethylamine

(10.12 g, 100.0 mmol) was added in portions to the ice-bath solution. The mixture was allowed to stir at room temperature for 18 hours. The solution solvent was evaporated *in vacuo* and ethyl ether (100 ml) was added to the residue. The solution was filtered and washed with water, 1N NaOH, 1N HCl and water. The solid was successively washed with DCM and ethyl acetate to obtain UA62784 amide (12.7 g, 34.2 mmol, 68.4 % yield). ¹H NMR (CDCl₃) 3.94 (s, 3 H), 5.02 (d, *J* = 4.5 Hz, 2 H), 7.03 (d, *J* = 9.0 Hz, 2 H), 7.16 (brs, 1 H, NH), 7.34-7.50 (m, 3 H), 7.64 (d, *J* = 7.8 Hz, 1 H), 7.72 (d, *J* = 7.5 Hz, 1 H), 7.79 (d, *J* = 7.5 Hz, 1 H), 7.87 (d, *J* = 8.1 Hz, 1 H), 8.05 (d, *J* = 9.0 Hz, 2 H) ppm.

Phosphorus oxychloride (12.39 g, 81.0 mmol) was added dropwise to a solution of UA62784 amide (10.0 g, 26.9 mmol) in DMF (200 ml). The mixture was heated to 90°C for 30 min and then poured into iced water (200 ml). The solution was extracted with DCM (200 ml) and combined organic phases were washed with water and brine, dried, and concentrated and washed with 20% DCM in hexane to obtain UA62784 (6.74 g, 19.07 mmol, 70.8 % yield) as a yellow solid. ¹H NMR (CDCl₃) 3.89 (s, 3 H), 7.02 (d, *J* = 8.7 Hz, 2 H), 7.36-7.52 (m, 4 H), 7.71 (d, *J* = 9.0 Hz, 2 H), 7.75 (d, *J* = 7.5 Hz, 1 H), 7.82 (d, *J* = 6.5 Hz, 1 H), 8.08 (d, *J* = 6.9 Hz, 1 H), 8.58 (d, *J* = 7.8 Hz, 1 H) ppm. ¹³C NMR (75 MHz, CDCl₃) 55.81, 114.96, 120.83, 122.27, 123.88, 124.53, 125.88, 126.07, 126.30, 129.29, 129.92, 134.70, 135.40, 135.99, 136.16, 142.37, 144.14, 152.25, 159.11, 160.56, 193.63 ppm. HRMS (M + H)⁺ calcd for C₂₃H₁₆NO₃ 354.1130; found 354.1140.

Cell Culture

Human pancreatic adenocarcinoma cell lines (BxPC3, MiaPaCa, and Pand-1) were purchased from the American Type Culture Collection (Manassas, VA) and grown in RPMI supplemented with 10% Bovine Calf Serum (BCS) (Hyclone; Logan, UT), 50 units/mL Penicillin and 50ug/mL Streptomycin (Invitrogen; Carlsbad, California), and 2 mM L-Glutamine (Invitrogen). Human foreskin fibroblast cells were established from fresh tissues at the Arizona Cancer Center (courtesy of the tissue culture shared service at Arizona Cancer Center). All cultures were incubated at 37°C in a humidified incubator with 5% CO₂.

MTT Viability Assay and Apoptosis

The MTT assay measures mitochondrial activity in viable cells based on the ability to convert 3-(4,5-dimethylthiazol-2-yl)-2,5-diphenyl tetrazolium bromide (MTT) to blue formazan (32). Cultured cells were seeded onto a 96-well microtiter plate. Cells were incubated with various amounts of UA62784 for 24, 48, 72, or 96 hours. At the end of the incubation, MTT solution (Thiazolyl Blue Tetrazolium Bromide, Sigma; St. Louis, MO) was added to each well at a final concentration of 0.2 mg/ml. The plates were incubated for 4 hours at 37°C in a humidified incubator, centrifuged briefly and aspirated. DMSO was added to each well to dissolve formazan crystals and allow for even color distribution. Absorbance was measured by a μ QuantTM Microplate Spectrophotometer (BioTek Instruments; Winooski, VT). The IC₅₀ values (defined as the drug concentration that inhibits cell growth by 50% of the control value) were determined by sigmoidal analysis using Origin 7.0 software (Northampton, MA).

To determine whether UA62784-treated cells undergo apoptosis, an Annexin V-FITC Apoptosis Detection Kit (BioVision Inc.; Mountain View, CA) was used. Briefly, cells were treated with UA62784 for 24 or 48 hours, harvested by trypsinization, and pelleted by centrifugation. All samples were resuspended in 1X binding buffer (BioVision Inc.). Propidium Iodide (PI) and Annexin V conjugated to Fluorescein Isothiocyanate (FITC) were added to each sample and samples were incubated for 5 minutes at room temperature. All samples were analyzed by flow cytometry using FITC signal detection and phycoerythrin emission signal detection (to detect PI).

Cell Cycle Analysis

Cells were incubated with UA62784 for 12 hrs. The cells were collected, washed with phosphate-buffered saline (PBS) (Invitrogen) and then fixed and permeabilized in 70% ethanol for at least 24 hours at -20°C. After incubation, pellets were rehydrated and incubated with primary antibody for 1 hour. Samples were then centrifuged, aspirated, and resuspended in PBS with secondary antibody for 30 minutes. Samples were washed as above and resuspended in PBS with 0.5 mg/ml RNase A and 0.04mg/ml propidium iodide (PI) (Sigma; St. Louis, MO). All samples were analyzed using a Becton Dickinson FACScan Flow Cytometer (Franklin Lakes, NJ).

The mitotic index measurement procedure was modified from Muehlbauer et al. (33). Briefly, cells were treated with UA62784, demecolcine (Sigma), or doxorubicin (Sigma), incubated with anti-phospho-Histone H3 and PI and analyzed by flow cytometry as above. All primary and secondary antibodies were used at dilutions recommended by the manufacturer. Phospho-Histone H3 (Ser10), phospho-cdc25C (Ser198), and phospho-cdc2 (Tyr15) antibodies were purchased from Cell Signaling Technology (Danvers, MA).

Microscopy

Cells were seeded into chamber slides or coverslips and allowed to attach overnight. Samples were treated with UA62784 for a predetermined amount of time. Samples were fixed using either 100% Methanol (tubulin samples) or 3.7% formaldehyde in PBS followed by 100% ethanol (non-tubulin samples). Samples were blocked with PBS-0.3% Triton-1% BCS.

Mouse anti- β -Tubulin was purchased from Sigma (St. Louis, MO). Rabbit anti-CENP-E was purchased from Cytoskeleton, Inc (Denver, CO). Mouse anti-BubR1 was purchased from AbCam (Cambridge, MA). Goat anti-mouse and goat anti-rabbit secondaries were purchased from Molecular Probes- Invitrogen (Carlsbad, CA). All antibody incubations were performed at concentrations recommended by the manufacturer. Primary antibodies were incubated overnight at 4°C and secondary antibodies were incubated for 1-2 hrs. at room temp. Slides were mounted using Vectashield Hard Set Mounting Medium with DAPI (Vector Laboratories; Burlingame, CA). Confocal images were visualized using a Nikon PCM2000 microscope and SimplePCI 6.0 software (Hamamatsu Corporation; Sewickley, PA).

Tubulin Polymerization Assay

Cell-free fluorescence-based tubulin polymerization kit and microtubule-associated protein (MAP) extract were purchased from Cytoskeleton, Inc. (Denver, CO). The assay was performed as indicated by manufacturer. All samples (wells) were prepared with 20% glycerol, 1 mM GTP, and 2 mg/ml tubulin monomers, except for MAP extract samples which contained 5% glycerol. Three (4) μ M Paclitaxel, 3 μ M Vincristine (Sigma), and various concentrations of UA62784 were added to pre-warmed plate prior to the addition of Tubulin Reaction Mix. The polymerization reaction was measured using a Gemini XPS Microplate Spectrofluorometer (Molecular Devices; Sunnyvale, CA). All time points were plotted and analyzed using SoftMax Pro® software (Molecular Devices).

Kinesin ATPase Assay

The colorimetric kinesin ATPase assay was purchased from Cytoskeleton, Inc and performed as indicated by manufacturer. In short, purified kinesin protein (0.2-1.0 μ g) (Cytoskeleton Inc.; Denver, CO) was added to Paclitaxel-stabilized microtubules in a 96-well plate. Various amounts of UA62784 were added to the wells prior to addition of ATP (Sigma; St. Louis, MO) and reaction was incubated at room temperature for 5 min. CytoPhos reagent (Cytoskeleton Inc.; Denver, CO) was added to halt the reaction and color was allowed to develop for 10 min.

Absorbance at 650 nm was measured by a μ Quant™ Microplate Spectrophotometer (BioTek Instruments; Winooski, VT).

Microtubule Binding and Polyacrylamide Gel Electrophoresis (PAGE)

The microtubule binding protein spin-down assay kit was purchased from Cytoskeleton, Inc. (Denver, CO) and completed as indicated by manufacturer. Briefly, purified taxol-stabilized microtubules were incubated at 37°C with microtubule binding proteins. Microtubule-associated protein (MAP) was used as a positive control for MT-binding and bovine serum albumin (BSA) (Sigma) was used for a negative control. Test samples had 1 μ g purified CENP-E motor protein (Cytoskeleton, Inc.) with varying concentrations of UA62784 (0-100 μ M). All samples were ultracentrifuged to pellet the MTs and aliquots were taken from the supernatant and pellet fractions.

All samples were boiled for 10 min. and run on a 10% SDS polyacrylamide gel. The resulting gel was either stained with Bio-Safe Coomassie (Bio-Rad Laboratories; Hercules, CA) as indicated by manufacturer or transferred to an Immobilon transfer membrane (Millipore; Billerica, MA). The membrane was blocked with Odyssey Blocking Buffer (Li-Cor Biosciences; Lincoln, NE), washed, and incubated with primary antibody diluted in 5% milk. Secondary antibodies were purchased from Li-Cor Biosciences. The membrane was incubated with secondary antibodies for 1 hr, washed, and analyzed using an Odyssey Infrared Imager and Odyssey 2.1 software (Li-Cor Biosciences).

Results

Effects of UA62784 on cell survival and apoptosis

To evaluate the *in vitro* cytotoxic activity of UA62784, we utilized the MTT assay to determine the IC₅₀. MiaPaCa, BxPC3, and Panc-1 cells were treated with various concentrations of UA62784 and incubated for 96 hours. The IC₅₀ value for each was calculated by sigmoidal analysis on a logarithmic curve. These results revealed varying sensitivities to UA62784 in the three cell lines, with MiaPaCa being the most sensitive (43.25 nM \pm 4.03), Panc-1 being intermediate (85 nM \pm 7.07) and BxPC3 being the least sensitive (103.8 nM \pm 14). Overall, all three cell lines were significantly more sensitive than primary foreskin fibroblast cells (IC₅₀>>50 μ M) and the lung embryonic fibroblast cell line IMR-90 (IC₅₀=3.13 μ M).

All three cell lines were analyzed for evidence of apoptosis by staining with Annexin-V-FITC and PI. Pancreatic cells were incubated with varying concentrations of UA62784 for 24 or 48 hours and analyzed by Flow Cytometry. In all cases, samples treated with 500 nM UA62784 and above showed evidence of apoptosis (as opposed to necrosis, indicated by staining for PI only) at both 24 and 48 hours (Figure S1).

UA62784 induces G2/M arrest

Flow Cytometric analysis was used to determine the effects of UA62784 on cell cycle progression in the three pancreatic cell lines (represented in figure 2). The MiaPaCa cell line exhibited a consistent G2/M arrest within 12 hours of incubation with 100nM of UA62784. The BxPC3 and Panc-1 cell lines also exhibited a G2/M arrest, but required treatment with 300 nM UA62784 for 12 hours before G2/M arrest was visible. Interestingly, treatment beyond 24 hours resulted in varying responses from the three cell lines. A high sub-G1 peak in MiaPaCa cells suggests that these cells undergo cell death following prolonged drug exposure. The BxPC3 cell line subverts the cell cycle block with prolonged exposure and continues cycling; producing an 8n peak which is visible after treating with 300nM UA62784 for 36 hours. After 48 hours of continuous treatment, Panc-1 cells appeared to remain arrested in G2/M, with no sub-G1 peaks and some slight accumulation of 8n cells (no significant peaks) appearing at the

highest drug concentration. In the cases of both BxPC3 and MiaPaCa cells the G1 peak completely disappeared following prolonged incubation with UA62784. Prolonged incubation in Panc-1 cells resulted in the G1 peak dropping from 56.2% (control) to 8.7% (300nM UA62784 for 36 hours).

The G2/M arrest induced by UA62784 is readily reversible over time as evidenced in figure 2. The MiaPaCa cells were treated with 100 nM UA62784 for 8 hours; enough to cause a G2/M arrest but not to cause apoptosis (Figure S1). These cells were then washed and allowed to recover in normal media for various amounts of time. After 1 hour of recovery, the G2/M peak had dropped significantly and appeared to have completely returned to a normal cell cycle distribution after only 3 hours of recovery.

Delineating the arrest stage, G2 or M

The flow cytometry experiments could not delineate if UA62784 was causing cell cycle arrest in the G2 or mitotic phase because total DNA content is the same for these two phases. Therefore, the expression of phospho-Histone H3 (Ser 10), a well-established mitotic marker (34), was examined by flow cytometry and fluorescence microscopy. Mitotic cells were defined as those with a 4n DNA content and positive staining for phospho-Histone H3.

MiaPaCa cells were treated for 8 hours with various amounts of UA62784 (Figure 3a). The mitotic population begins increasing at 100 nM and peaks at 500 μ M. Cells were also treated with demecolcine (a colchicine analog and known tubulin polymerization inhibitor) (Figure 3b) and doxorubicin (Figure 3c) to serve as positive and negative controls for mitotic inhibition, respectively. Demecolcine produced a substantial increase in the mitotic population as expected, whereas treatment with doxorubicin (a topoisomerase-II inhibitor) caused a decrease in the mitotic population. This was expected since Doxorubicin is known to inhibit cells in G1/G2 (35). Both Panc-1 and BxPC3 cells exhibited similar results showing arrest in early mitosis after exposure to UA62784 (data not shown).

To confirm these results, fluorescence microscopy was done using the same phospho-Histone H3 marker (Figure S2). Untreated cells showed only a small percentage of the total population in mitosis ($7.6\% \pm 1.7$). Additionally, all stages of mitosis were seen in untreated samples. Following treatment with UA62784, the mitotic population was significantly enriched ($41.5\% \pm 4.9$). Interestingly, it appeared that none of the treated cells had progressed into metaphase, as evidenced by a lack of chromosomal alignment at the metaphase plate. All of the treated cells that were in mitosis appeared to be in either prophase or prometaphase, as evidenced by the presence of condensed chromatin or lack thereof. Additionally, cells treated with UA62784 lacked a bipolar spindle. We therefore concluded that UA62784 causes mitotic arrest prior to metaphase.

UA62784 does not directly influence tubulin polymerization

Due to the lack of a functional mitotic spindle in UA62784-treated cells (Figure S3), we sought to determine if UA62784 affects tubulin polymerization. For this, we utilized a cell-free tubulin polymerization assay that relies on a fluorescence-based reporter system. Paclitaxel and vincristine were used as positive and negative controls, respectively. As shown in figure S4, UA62784 does not significantly affect tubulin polymerization, but the positive controls produced classic hyper-polymerization (paclitaxel) or blocked polymerization (vincristine).

Microtubule associated proteins (MAPs) are proteins that bind to tubulin to assist in polymerization and stabilization (36). Because inhibition of MAPs might have the same overall affect as a direct inhibition of tubulin, we repeated the tubulin polymerization assay with a MAP fraction added (which includes MAP1, MAP2, and tau proteins). Again, tubulin

polymerization assisted by MAPs was not significantly affected by the addition of UA62784 (data not shown).

CENP-E ATPase Activity and Localization

We next tested UA62784 for kinesin motor protein inhibition using a cell-free assay that relies on the formation of free inorganic phosphate following ATPase activity (37). Several kinesins were tested for UA62784-mediated inhibition, including Eg5, CENP-E, MKLP-1, KIF3C, and MCAK. Of these kinesins, UA62784 exhibited activity against only CENP-E, showing approximately 80% inhibition at the highest concentration tested (Figure 4).

We used immunofluorescence microscopy to visualize CENP-E localization in treated versus untreated cells (Figure 5). Untreated Panc-1 cells demonstrate a characteristic staining pattern (30) wherein CENP-E staining is absent in interphase cells but localizes to the cytoplasm during prophase, to the kinetochores during prometaphase/metaphase, and to the spindle midzone during anaphase. Cells treated with UA62784 demonstrated both prophase and prometaphase-type staining with CENP-E localizing to the cytoplasm and kinetochores (respectively). However, all treated cells appeared to have kinetochores that were scattered throughout to nucleus as opposed to lining up at the metaphase plate, confirming our results that UA62784 arrests cells prior to metaphase.

Because the kinesin inhibitor Adociasulfate-2 acts by preventing kinesin motor binding to MTs (25,38), we sought to determine if UA62784 acts by a similar mechanism. A microtubule pull-down assay was performed to visualize CENP-E binding in the presence and absence of UA62784 (Figure 6). Proteins that bind to microtubules should be apparent in the pellet portion of each sample when subjected to PAGE analysis. Microtubule-associated protein fraction (MAPF) and bovine serum albumin (BSA) were used as positive and negative controls (respectively) for MT binding. When run on a PAGE gel and stained with coomassie, we see that MAPF proteins appear in the pellet fraction whereas BSA appears in the supernatant fraction. Adding increasing amounts of UA62784 did not alter the amount of CENP-E within the pellet fraction, therefore we conclude that UA62784 does not affect CENP-E binding to MTs.

The CENP-E kinesin is known to associate with BubR1 at unattached kinetochores to facilitate spindle checkpoint signaling (39,40). To determine if UA62784 affects the colocalization of BubR1 and CENP-E at the kinetochore during mitosis we treated Panc-1 cells with 500nM UA62784 or an equal volume of DMSO. As shown in figure S5, both control and treated cells show colocalization of BubR1 and CENP-E, indicating that UA62784 does not affect the association of CENP-E and BubR1 at the kinetochore.

Discussion

These results show that UA62784 induces mitotic arrest and apoptosis in pancreatic carcinoma cell lines. Although this compound was originally isolated from a screen designed to identify compounds that would selectively target DPC4-deleted cells, it should be noted that of the cell lines used in our experiments, only BxPC3 cells have the DPC4 gene deletion. Both MiaPaCa and Panc-1 cells have a wild-type DPC4 gene. Therefore, DPC4 status alone does not seem to directly correlate with sensitivity to UA62784. However, there was an increase in the percentage of apoptotic cells in BxPC3 (DPC4⁻) vs. BxPC3 (DPC4⁺) cells treated with UA62784 (data not shown), confirming the initial modest selectivity for DPC4⁻ cells. Additionally, we noticed that UA62784 has greater cytotoxic potency in pancreatic carcinoma cell lines when compared to normal fibroblast cells.

The mitotic arrest seen in these pancreatic cancer cell lines can be explained by the inhibition of an essential mitotic protein. Specifically, UA62784 acts on the CENP-E kinesin-like protein by inhibiting its microtubule-associated ATPase activity. Conversely, the agent does not affect the ability of CENP-E to bind to microtubules nor its localization in the mitotic cell. Inhibition of CENP-E is known to cause mitotic arrest prior to metaphase due to lack of chromosomal congression at the metaphase plate. Cells treated with UA62784 were viewed using immunofluorescent confocal microscopy and were seen to be arrested in either prophase or prometaphase, but almost never in metaphase or anaphase. This is consistent with studies showing that the depletion of CENP-E is known to cause aneuploidy in some models (41). Indeed, we saw evidence of 8n populations in both MiaPaCa and BxPC3 cells when screening for UA62784 effects on total DNA content using flow cytometry (data not shown).

When screened against a panel of five different kinesin motor proteins, UA62784 showed inhibition of ATPase activity only in the CENP-E motor protein. Although there appears to be some disparity between the *in vitro* IC₅₀ for UA62784 and the concentration required for inhibition of the purified protein, we note that previous trials with the kinesin ATPase assay required similar increases in drug concentration to elicit measurable ATPase inhibition (37). This is likely due to the fact that CENP-E kinesin protein concentrations in the cell are significantly lower than that required for the assay (42).

Though UA62784 holds promise in treating certain types of pancreatic (and presumably other) cancers, further analog development is probably needed due to its lack of aqueous solubility. Also, we believe a more broad-spectrum mitotic kinesin inhibitor may impart better tumor inhibition due to the redundancy seen in the function of some mitotic kinesins. These studies can be optimized to isolate compounds specific only for mitotic kinesins (such as Eg5 and CENP-E) and not neuronal kinesins (such as KIF3C). We have already developed several chemical analogs of UA62784 with improved aqueous solubility and are working to further characterize the kinesin inhibition patterns for possible clinical development. Several other kinesin inhibitors developed by other groups are currently being evaluated for clinical antitumor efficacy including two KSP/Eg5 kinesin inhibitors ispinesib (43,44) and SB-743921 (45). To date, these inhibitors have shown limited efficacy in the clinic, underscoring the importance for continued development of alternative mitotic kinesin inhibitors that target molecules other than EG5.

Supplementary Material

Refer to Web version on PubMed Central for supplementary material.

Acknowledgements

This work was supported by the Pancreatic Program Project Grant (CA109552).

Financial Support: Pancreatic Program Project Grant (CA109552)

Abbreviations

CENP-E, centromere protein E; DPC4, deleted in pancreatic cancer 4; AK, aurora kinase; PI, propidium iodide; MT, microtubule; MAP, microtubule-associated protein.

References

1. Jemal A, Siegel R, Ward E, et al. Cancer statistics, 2008. *CA Cancer J Clin* Mar-Apr;2008 58(2):71–96. [PubMed: 18287387]

2. Zalutnai A. Novel therapeutic approaches in the treatment of advanced pancreatic carcinoma. *Cancer Treatment Reviews* 2007;33:289–98. [PubMed: 17343986]
3. Carmichael J, Fink U, Russell RC, Spittle MF, Harris AL, Spiessi G, Blatter J. Phase II study of gemcitabine in patients with advanced pancreatic cancer. *British Journal of Cancer* 1996;73(1):101–5. [PubMed: 8554969]
4. Burris HA 3rd, Moore MJ, Andersen J, et al. Improvements in survival and clinical benefit with gemcitabine as first-line therapy for patients with advanced pancreas cancer: a randomized trial. *J Clin Oncol Jun*;1997 15(6):2403–13. [PubMed: 9196156]
5. Cascinu S, Gasparini G, Catalano V, Silva RR, Pancera G, Morabito A, Giordani P, Gattuso D, Catalano G. A phase I-II study of gemcitabine and docetaxel in advanced pancreatic cancer: a report from the Italian Group for the Study of Digestive Tract Cancer (GISCAD). *Annals of Oncology* 1999;10(11):1377–9. [PubMed: 10631469]
6. Jacobs AD. Gemcitabine-based therapy in pancreas cancer: gemcitabinedocetaxel and other novel combinations. *Cancer Aug 15*;2002 95(4 Suppl):923–7. [PubMed: 12209672]
7. Ridwelski K, Fahlke J, Kuhn R, et al. Multicenter phase-I/II study using a combination of gemcitabine and docetaxel in metastasized and unresectable, locally advanced pancreatic carcinoma. *Eur J Surg Oncol Apr*;2006 32(3):297–302. [PubMed: 16414235]
8. Gopalan G, Chan CS, Donovan PJ. A novel mammalian, mitotic spindle-associated kinase is related to yeast and fly chromosome segregation regulators. *Journal of Cell Biology* 1997;138(3):643–56. [PubMed: 9245792]
9. Harrington EA, Bebbington D, Moore J, Rasmussen RK, Ajose-Adeogun AO, Nakayama T, Graham JA, Demur C, Hercend T, Diu-Hercend A, Su M, Golec JM, Miller KM. VX-680, a potent and selective small-molecule inhibitor of the Aurora kinases, suppresses tumor growth in vivo. *Nature Medicine* 2004;10(3):262–7.
10. Rudner AD, Murray AW. The spindle assembly checkpoint. *Current Opinion in Cell Biology* 1996;8:773–80. [PubMed: 8939672]
11. Pinsky BA, Biggins S. The spindle checkpoint: tension versus attachment. *Trends in Cell Biology* 2005;15(9):486–93. [PubMed: 16084093]
12. Rieder CL, Schultz A, Cole R, Sluder G. Anaphase onset in vertebrate somatic cells is controlled by a checkpoint that monitors sister kinetochore attachment to the spindle. *Journal of Cell Biology* 1994;127(5):1301–10. [PubMed: 7962091]
13. Li XaN RB. Mitotic forces control a cell-cycle checkpoint. *Nature* 1995;373(6515):630–2. [PubMed: 7854422]
14. Gotaskie GE, Andreassi BF. Paclitaxel: a new antimitotic chemotherapeutic agent. *Cancer Practice* 1994;2(1):27–33. [PubMed: 7914453]
15. Zhou XJ, Rahmani R. Preclinical and clinical pharmacology of vinca alkaloids. *Drugs* 1992;44:66–9.
16. Roy SN, Horwitz SB. A phosphoglycoprotein associated with taxol resistnace in J774.2 cells. *Cancer Research* 1985;45(8):3856–63. [PubMed: 2861892]
17. Golsteyn RM, Mundt KE, Fry AM, Nigg EA. Cell cycle regulation of the activity and subcellular localization of Plk1, a human protein kinase implicated in mitotic spindle function. *Journal of Cell Biology* 1995;129(6):1617–28. [PubMed: 7790358]
18. Sawin KE, LeGuellec K, Philippe M, Mitchison TJ. Mitotic spindle organization by a plus-end-directed microtubule motor. *Nature* 1992;359(6395):540–3. [PubMed: 1406972]
19. Miglarese MRaC RO. Development of new cancer therapeutic agents targeting mitosis. *Expert Opinion on Investigational Drugs* 2006;15(11):1411–25. [PubMed: 17040200]
20. Mayer TU, Kapoor TM, Haggarty SJ, King RW, Schreiber SL, Mitchison TJ. Small molecule inhibitor of mitotic spindle bipolarity identified in a phenotype-based screen. *Science* 1999;286:971–4. [PubMed: 10542155]
21. Kapoor TM, Mayer TU, Coughlin ML, Mitchison TJ. Probing spindle assembly mechanisms with Monastrol, a small molecule inhibitor of the mitotic kinesin, Eg5. *The Journal of Cell Biology* 2000;150(5):975–88. [PubMed: 10973989]
22. Koller E, Propp S, Zhang H, Zhao C, Xiao X, Chang M, Hirsch SA, Shepard PJ, Koo S, Murphy C, Glazer RI, Dean NM. Use of a chemically modified antisense oligonucleotide library to identify and

- validate Eg5 (Kinesin-like 1) as a target for antineoplastic drug development. *Cancer Research* 2006;66(4):2059–66. [PubMed: 16489005]
23. Carter BZ, Mak DH, Shi Y, Schober WD, Wang RY, Konopleva M, Koller E, Dean NM, Andreef M. Regulation and targeting of Eg5, a mitotic motor protein in blast crisis CML: overcoming imatinib resistance. *Cell Cycle* 2006;5(19):2223–9. [PubMed: 16969080]
 24. Saio T, Ishii G, Ochiai A, Yoh K, Goto K, Nagai K, Kato H, Nishiwaki Y, Saijo N. Eg5 expression is closely correlated with the response of advanced non-small cell lung cancer to antimetabolic agents combined with platinum chemotherapy. *Lung Cancer* 2006;54(2):217–25. [PubMed: 16934364]
 25. Sakowicz R, Berdelis MS, Ray K, Blackburn CL, Hopmann C, Faulkner DJ, Goldstein LSB. A marine natural product inhibitor of kinesin motors. *Science* 1998;280:292–5. [PubMed: 9535660]
 26. Wood KW, Sakowicz R, Goldstein LSB, Cleveland DW. CENP-E is a plus end-directed kinetochore motor required for metaphase chromosome alignment. *Cell* 1997;91:357–66. [PubMed: 9363944]
 27. Schaar BT, Chan GKT, Maddox P, Salmon ED, Yen TJ. CENP-E function at kinetochores is essential for chromosome alignment. *Journal of Cell Biology* 1997;139(6):1373–82. [PubMed: 9396744]
 28. Chan GKT, Jablonski SA, Sudakin V, Hittle JC, Yen TJ. Human BUBR1 is a mitotic checkpoint kinase that monitors CENP-E functions at kinetochores and binds the cyclosome/APC. *Journal of Cell Biology* 1999;146(5):941–54. [PubMed: 10477750]
 29. Yao X, Abrieu A, Zheng Y, Sullivan KF, Cleveland DW. CENP-E forms a link between attachment of spindle microtubules to kinetochores and the mitotic checkpoint. *Nature Cell Biology* 2000;2:484–91.
 30. Yen TJ, Compton DA, Wise D, Zinkowski RP, Brinkley BR, Earnshaw WC, Cleveland DW. CENP-E, a novel human centromere-associated protein required for progression from metaphase to anaphase. *The EMBO Journal* 1991;10(5):1245–54. [PubMed: 2022189]
 31. Wang H, Han H, VonHoff DD. Identification of an agent selectively targeting DPC4 (deleted in pancreatic cancer locus 4)-deficient pancreatic cancer cells. *Cancer Research* 2006;66(19):9722–30. [PubMed: 17018631]
 32. Mosmann T. Rapid colorimetric assay for cellular growth and survival: application to proliferation and cytotoxicity assays. *Journal of Immunological Methods* 1983;65:55–63. [PubMed: 6606682]
 33. Muehlbauer PA, Schuler MJ. Measuring the mitotic index in chemically-treated human lymphocyte cultures by flow cytometry. *Mutat Res Jun* 6;2003 537(2):117–30. [PubMed: 12787817]
 34. Juan G, Traganos F, James WM, Ray JM, Roberge M, Sauve DM, Anderson H, Darzynkiewicz Z. Histone H3 phosphorylation and expression of cyclins A and B1 measured in individual cells during their progression through G2 and mitosis. *Cytometry* 1998;32:71–7. [PubMed: 9627219]
 35. Krishan AaF E. Effect of adriamycin on the cell cycle traverse and kinetics of cultured human lymphoblasts. *Cancer Research* 1976;36(1):143–50. [PubMed: 1247994]
 36. Maccioni RBaC V. Role of microtubule-associated proteins in the control of microtubule assembly. *Physiological Reviews* 1995;75(4):835–64. [PubMed: 7480164]
 37. Funk CJ, Davis AS, Hopkins JA, Middleton KM. Development of high-throughput screens for discovery of kinesin adenosine triphosphatase modulators. *Annalytical Biochemistry* 2004;329(1):68–76.
 38. Brier S, Carletti E, DeBonis S, Hewat E, Lemaire D, Kozielski F. The marine natural product Adociasulfate-2 as a tool to identify the MT-binding region of kinesins. *Biochemistry* 2006;45:15644–53. [PubMed: 17176086]
 39. Mao Y, Desai A, Cleveland DW. Microtubule capture by CENP-E silences BubR1-dependent mitotic checkpoint signaling. *J Cell Biol Sep* 12;2005 170(6):873–80. [PubMed: 16144904]
 40. Chan GK, Jablonski SA, Sudakin V, Hittle JC, Yen TJ. Human BUBR1 is a mitotic checkpoint kinase that monitors CENP-E functions at kinetochores and binds the cyclosome/APC. *J Cell Biol Sep* 6;1999 146(5):941–54. [PubMed: 10477750]
 41. Weaver BAA, Silk AD, Montagna C, Verdier-Pinard P, Cleveland D. Aneuploidy acts both oncogenically and as a tumor suppressor. *Cancer Cell* 2007;11:25–36. [PubMed: 17189716]
 42. Brown KD, Coulson RM, Yen TJ, Cleveland DW. Cyclin-like accumulation and loss of the putative kinetochore motor CENP-E results from coupling continuous synthesis with specific degradation at the end of mitosis. *The Journal of Cell Biology* 1994;125(6):1303–12. [PubMed: 8207059]

43. Lee CW, Belanger K, Rao SC, et al. A phase II study of ispinesib (SB-715992) in patients with metastatic or recurrent malignant melanoma: a National Cancer Institute of Canada Clinical Trials Group trial. *Invest New Drugs* Jun;2008 26(3):249–55. [PubMed: 17962907]
44. Blagden SP, Molife LR, Seebaran A, et al. A phase I trial of ispinesib, a kinesin spindle protein inhibitor, with docetaxel in patients with advanced solid tumours. *Br J Cancer* Mar 11;2008 98(5): 894–9. [PubMed: 18319713]
45. O'Connor, O.; Goy, A.; Orłowski, R., et al. Phase I-II Study to Determine the Safety, Pharmacokinetics and Potential Efficacy of the Kinesin Spindle Protein (KSP) Inhibitor SB-743921 on Days 1 and 15 of a 28 Day Schedule in Patients with Non-Hodgkin's or Hodgkin's Lymphoma. 49th American Society of Hematology Annual Meeting; Atlanta, GA. 2007 December; 2007.

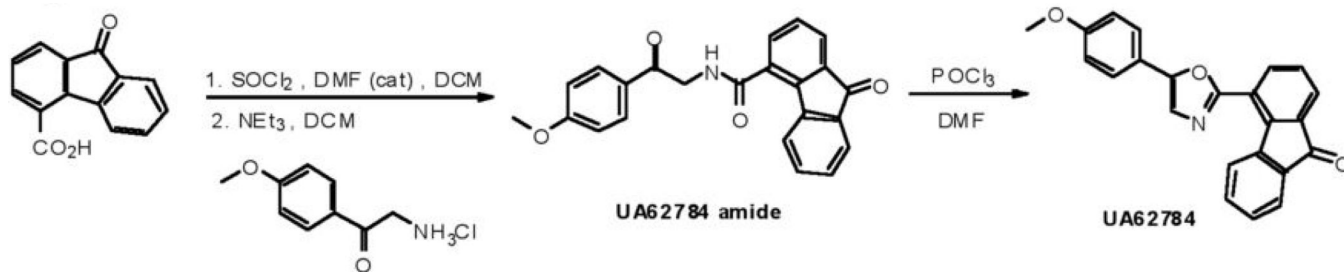


Figure 1.
Synthesis of UA62784

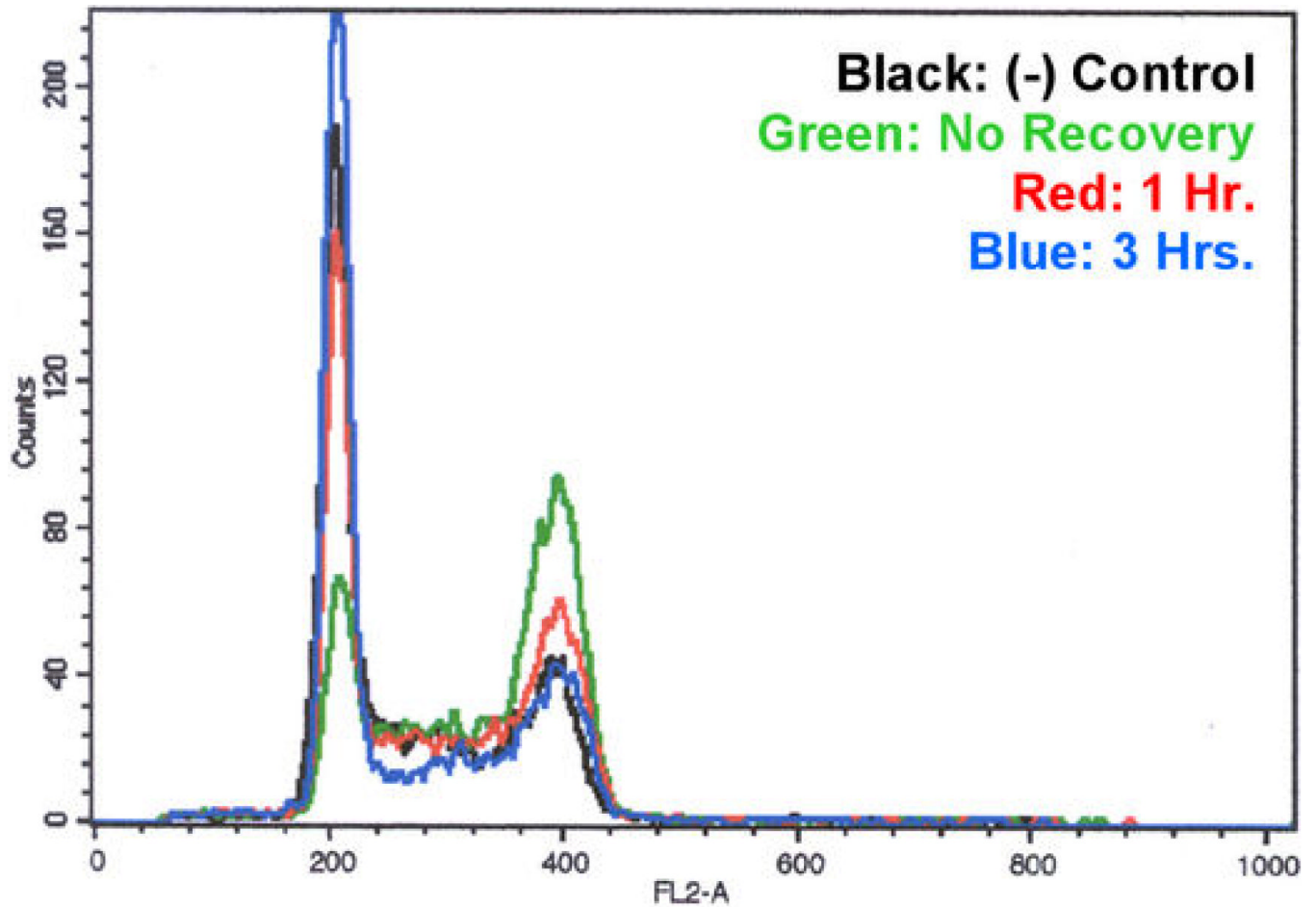


Figure 2.

Flow cytometric cell cycle analysis following recovery from UA62784 treatment. MiaPaCa cells were treated with UA62784 for 8 hrs. and allowed to recover in fresh media for the indicated amount of time. The cells were harvested, incubated with PI and analyzed by flow cytometry. The results show a loss of G2/M accumulation (far right peak) and a gain of the G1 population (left peak) over time.

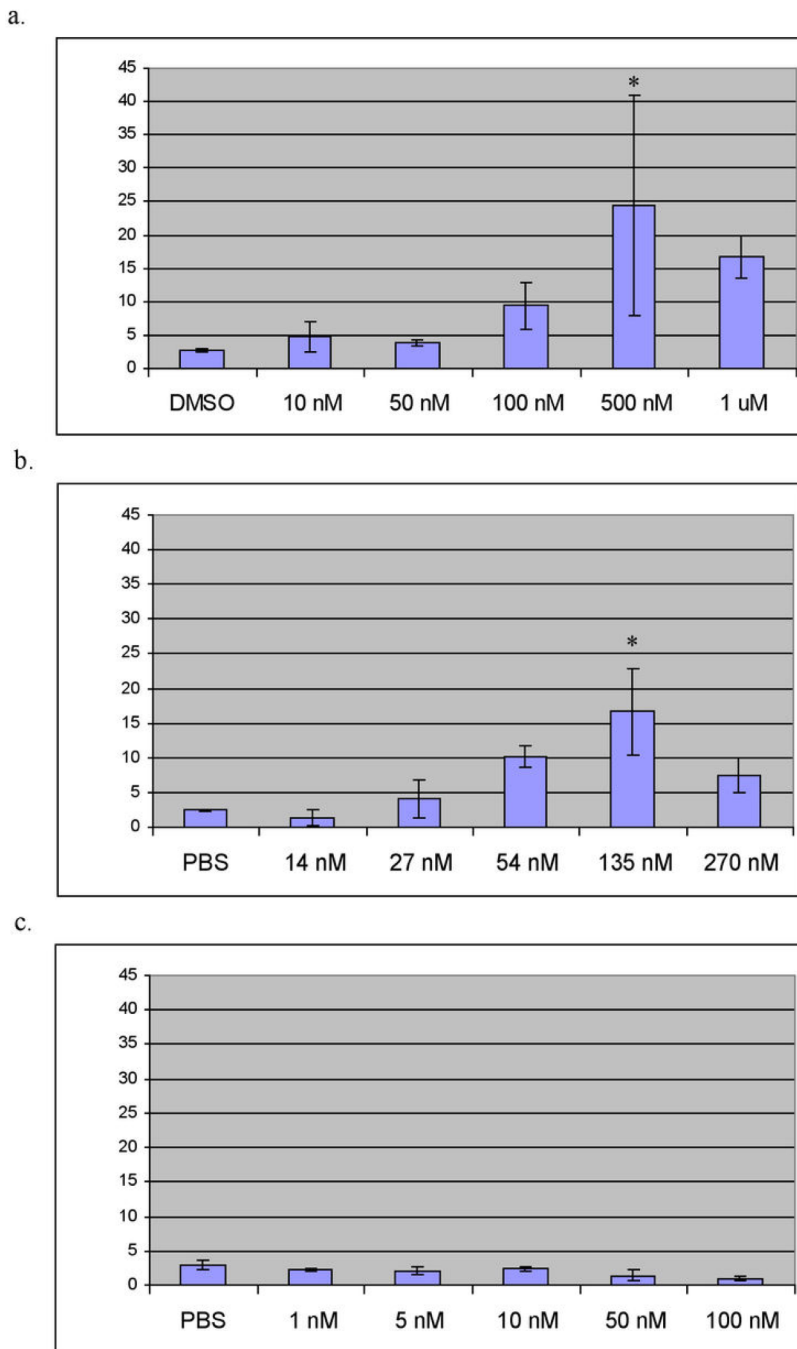


Figure 3. Mitotic index in cells treated with UA62784. Cells were incubated with the indicated amounts of UA62784 for 8 hours (a), Demecolcine for 24 hours (b), or Doxorubicin for 12 hours (c). Cells were harvested and incubated with an anti-phospho-Histone H3 antibody and propidium iodide (PI). Samples were analyzed by flow cytometry to quantify the mitotic index, indicated by a 4n DNA content and positive staining for phospho-Histone-H3. Error bars shown in (a) and (b) represent standard deviation (n=3). Asterisks indicate statistically significant results (p=0.05).

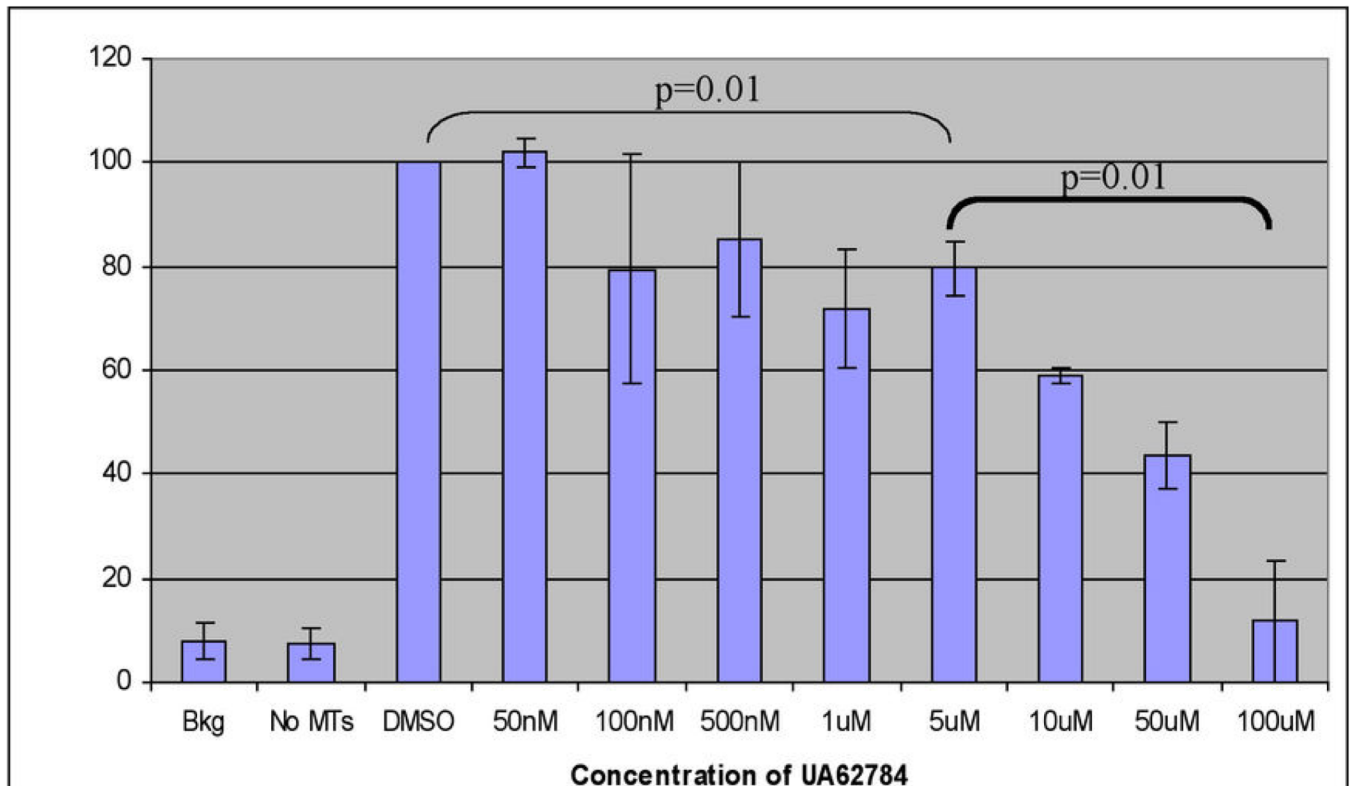


Figure 4.

Kinesin ATPase assay using CENP-E purified motor domain protein. ATPase activity was measured by generation of Pi following addition of ATP and taxol-stabilized MTs to purified kinesin motor protein. Bkg- Background; no ATP added, No MTs- no microtubules added to reaction, DMSO-negative control, no UA62784 added. Error bars are shown to indicate standard deviation (n=4).

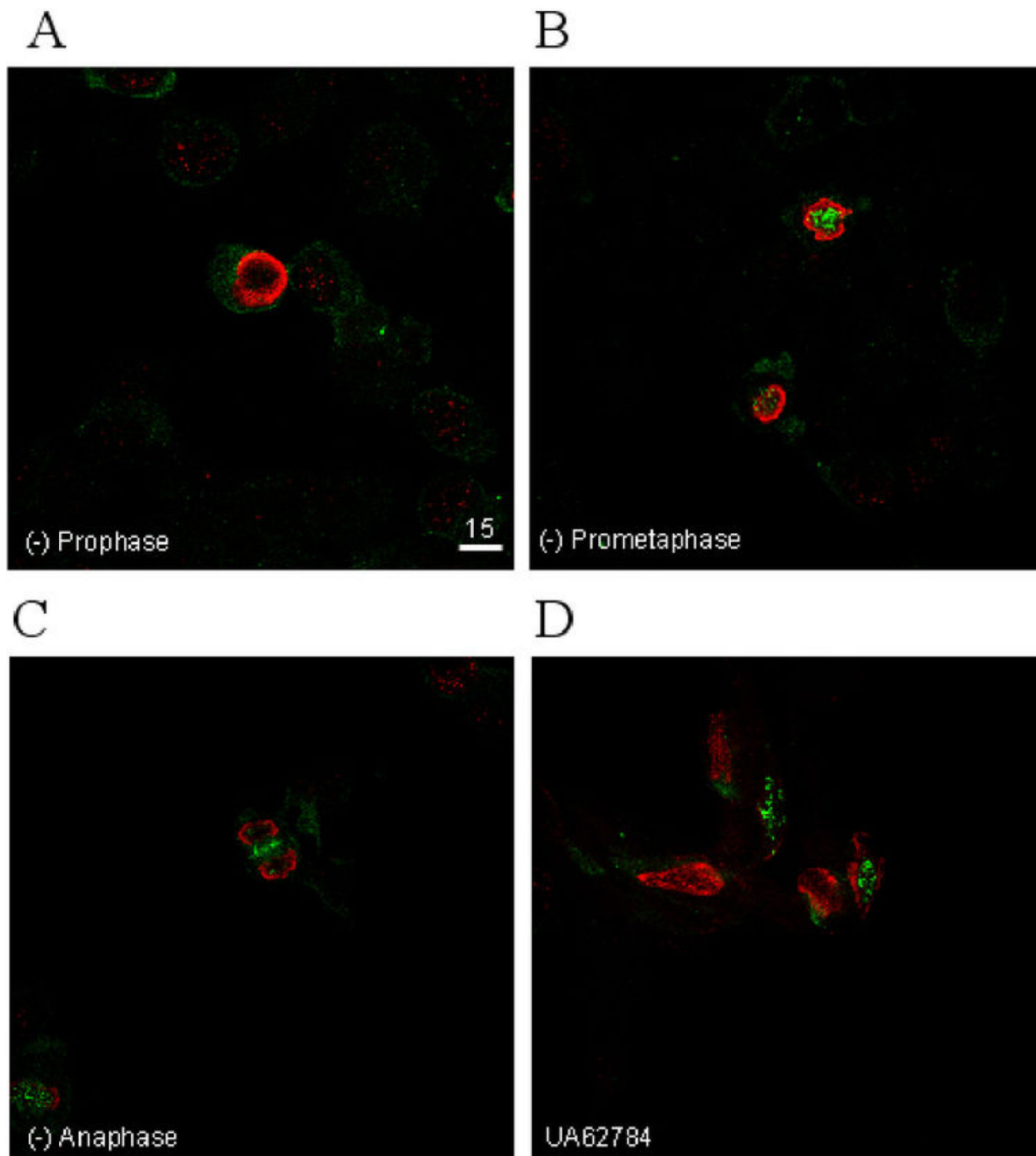


Figure 5. Immunofluorescent confocal microscopy (40X) staining for phospho-Histone H3 (red), a mitotic marker, and CENP-E (4). Panc-1 cells were left untreated (a-c) or were treated with 500nM UA62784 for 12 hrs. (d). Progression through mitosis is shown in a-c with CENP-E localizing diffusely in the cytoplasm during prophase (a), localizing to the DNA/kinetochores during prometaphase/metaphase (b), and localizing to the spindle midzone during anaphase (c). All cells in (a-c) are representative of one untreated sample. Note: only one cross-section of each confocal image is shown. These data are representative of 3 independent trials.

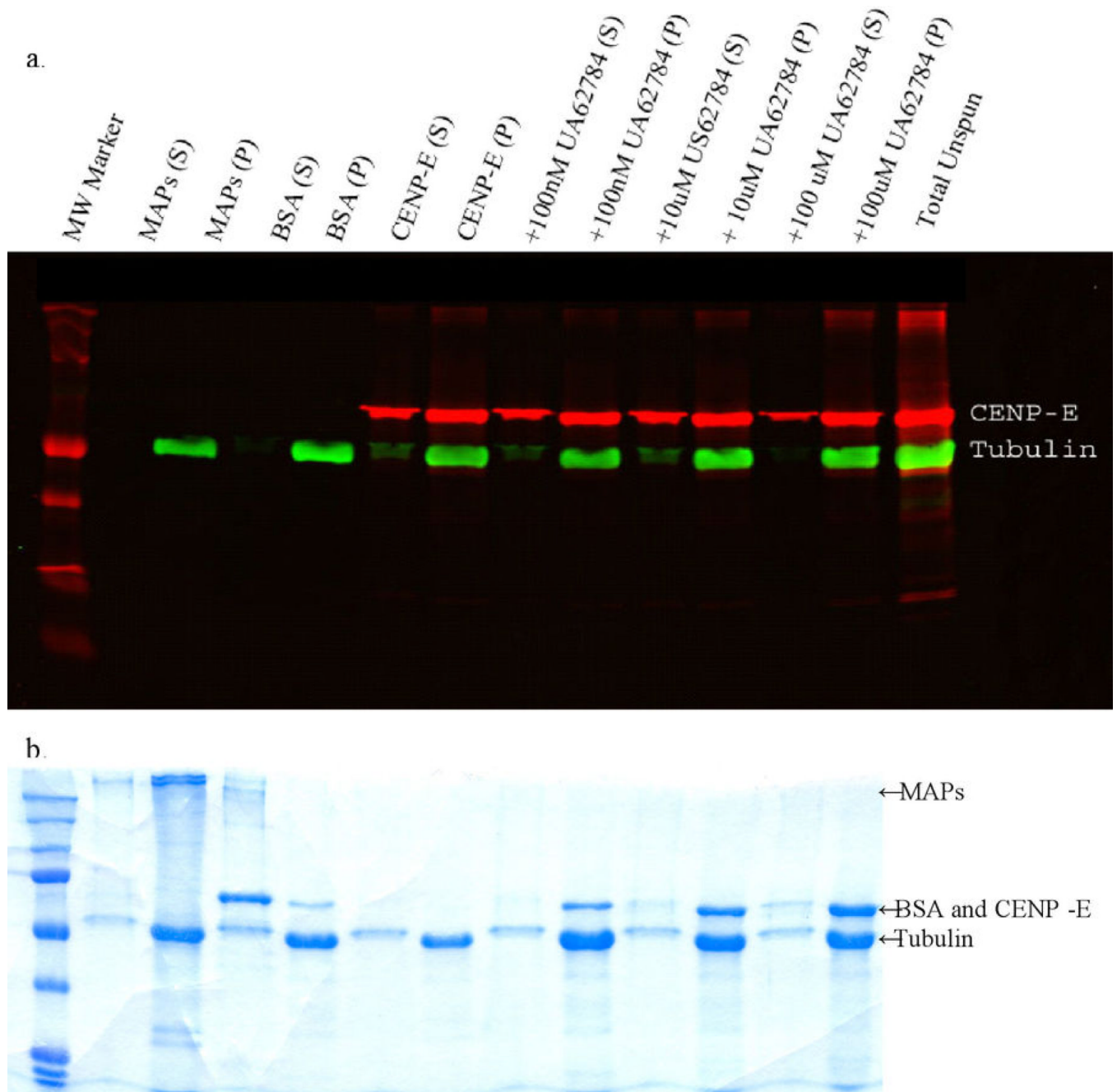


Figure 6. CENP-E microtubule-binding assay in the presence of UA62784. Purified taxol-stabilized microtubules were incubated with microtubule-associated protein extract (lanes 2-3), bovine serum albumin (4-5), CENP-E (6-7), or CENP-E and indicated concentrations of UA62784 (8-13) and ultracentrifuged to pellet microtubules. Any proteins that bind microtubules would be found primarily in the pellet (P) fraction whereas proteins that do not bind microtubules would be found primarily in the supernatant (S) fraction. Blots were visualized using IR secondaries (a) to indicate CENP-E and tubulin proteins only and Coomassie Blue staining (b) to indicate total protein. These data are representative of 4 independent experiments.